IOP PUBLISHING JOURNAL OF PHYSICS: CONDENSED MATTER

J. Phys.: Condens. Matter **19** (2007) 205131 (12pp) doi:10.1088/0953-8984/19/20/205131

Short- and long-range correlated motion observed in colloidal glasses and liquids

Eric R Weeks[1], **John C Crocker**[2] **and D A Weitz**[3]

[1] Physics Department, Emory University, Atlanta, GA 30322, USA
[2] Department of Chemical and Biomolecular Engineering, University of Pennsylvania, Philadelphia, PA 19102, USA
[3] Department of Physics and DEAS, Harvard University, Cambridge, MA 02138, USA

E-mail: weeks@physics.emory.edu

Received 6 October 2006
Published 25 April 2007
Online at stacks.iop.org/JPhysCM/19/205131

Abstract

We use a confocal microscope to examine the motion of individual particles in a dense colloidal suspension. Close to the glass transition, particle motion is strongly spatially correlated. The correlations decay exponentially with particle separation, yielding a dynamic length scale of O(2–3σ) (in terms of particle diameter σ). This length scale grows modestly as the glass transition is approached. Further, the correlated motion exhibits a strong spatial dependence on the pair correlation function $g(r)$. Motion within glassy samples is weakly correlated, but with a larger spatial scale for this correlation.

1. Introduction

The viscosity of a glass-forming material increases rapidly by many orders of magnitude as it is cooled, without any corresponding structural change to account for the viscosity change [1, 2]. Adam and Gibbs suggested that a growing dynamic length scale may relate to the viscosity growth [3]. Their idea has been interpreted in several ways [1, 2, 4–8], but no experiment has been able to observe dynamic length scales directly, nor is it clear what form these length scales would take. Indirect evidence is provided by experiments which locally perturb materials in a variety of ways, and observe the relaxation response of the material and its dependence on the scale of the perturbation [9]. Further evidence for a dynamic length scale comes from experiments performed in thin films or small pores [10], but these experiments do not observe the nature of any correlated motion directly. Recent simulations examined correlation functions in systems of Lennard-Jones particles [11, 12] and hard spheres [13], finding evidence for spatial correlations and a possible dynamical correlation length scale [11, 13].

We study a system of colloidal particles which interact only via repulsive forces, and which have a glass transition as their concentration is increased. We use a confocal microscope to track the motions of several thousand particles for several hours, which is long enough

for most particles to undergo non-trivial displacements. The mobilities of these particles (the magnitudes of their displacements) are correlated over distances of ∼2–4σ, in terms of the particle diameter σ. These correlations reflect large-scale cooperative rearrangements of particles seen previously [11, 13–16]. We also examine the correlations between the directions of particle displacements. While the directions are correlated, this does not appear to be as strong a signature of the rearrangements. These measurements are direct experimental studies of the nature of the long-range correlations present near a glass transition, and indicate that rearranging regions of particles are composed of particles with large displacements, but which do not all move in similar directions; rather, these regions are internally rearranging [17].

2. Experimental methods

Our system consists of a suspension of colloidal poly-methyl-methacrylate, sterically stabilized and dyed with a rhodamine dye [18]. These particles are slightly charged, and have a hard-sphere diameter $\sigma = 2.36$ μm and a polydispersity of 5%. They are suspended in a mixture of cycloheptylbromide and decalin which nearly index and density matches the particles. The samples are prepared with a constant volume fraction ϕ and sealed into microscope chambers. We observe crystallization occurring at $\phi = 0.42$, slightly lower than the value expected for hard spheres ($\phi_{\mathrm{HS}} = 0.494$) [19, 20]. Samples with $\phi > \phi_{\mathrm{g}} \approx 0.58$ do not form crystals within the bulk, even after sitting at rest for several months, allowing us to identify ϕ_{g} as the glass transition volume fraction, in agreement with previous work [19, 20]. Prior to observation, samples with crystals in them are shear-melted by means of a stir bar; there is a reasonable separation of timescales between the decay of transient flows caused by the stirring (<20 min) and the onset of crystallization for these samples (>5–10 h, as determined by methods described in [21]).

We use confocal microscopy to observe the particle motion. A single three-dimensional image is acquired in 10 s, and over the course of an experiment we acquire several hundred images. As the mean square displacement curves show in figure 1(a), particles do not move significant distances on a timescale of 10 s. We post-process the data to determine particle positions with an accuracy of 0.03 μm horizontally and 0.05 μm vertically [18]. Each three-dimensional image is 69 μm × 65 μm × 14 μm and contains several thousand particles. We focus at least 25 μm from the cover slip to avoid interference from the wall, and in fact the observed motion appears to be isotropic.

3. Results

To characterize the behaviour of the samples, we calculate the particles' mean square displacement $\langle \Delta x^2 \rangle$, shown in figure 1(a) for five samples. These curves all show a plateau, due to cage-trapping: each particle is confined in a cage formed by its neighbours. At longer times, $\langle \Delta x^2 \rangle$ shows an upturn, indicating that at least some particles have moved. For the supercooled fluids (thick lines, $\phi < \phi_{\mathrm{g}}$), previous work showed that these motions correspond to a small subset of particles undergoing cage rearrangements [11, 14–16]. These particles move significantly further than the majority of the particles, and thus distributions of the particle displacements show broad tails at these timescales [11, 14–16]. This is quantifiable by the non-Gaussian parameter

$$\alpha_2(\Delta t) = \frac{\langle \Delta x^4 \rangle}{3\langle \Delta x^2 \rangle^2} - 1 \tag{1}$$

where the moments of Δx are calculated from the measured distributions of the one-dimensional displacements Δx. α_2 is zero for a Gaussian, and larger when the distributions

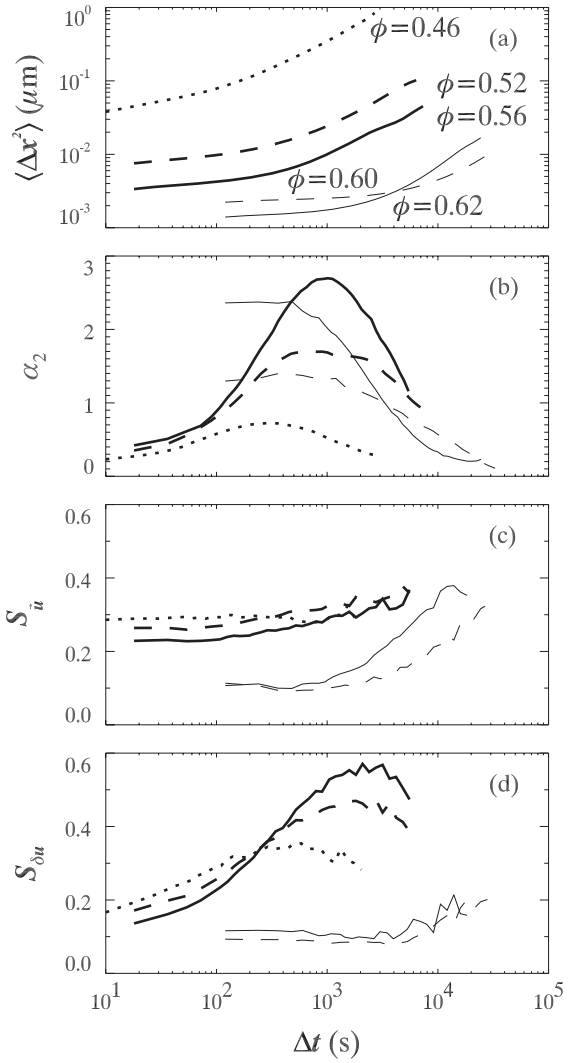

Figure 1. (a) Mean square displacement for colloidal 'supercooled' fluids (thick lines) and colloidal glasses, with volume fractions ϕ as labelled. (b) Non-Gaussian parameter α_2 for the samples shown in (a). (c), (d) Vector correlation function $S_{\vec{u}}(\Delta t)$ and scalar correlation function $S_{\delta u}(\Delta t)$ for the samples shown in (a), using Δr corresponding to the first peak of the peak of $g(r)$ for each sample.

are broader than a Gaussian. We plot α_2 in figure 1(b), finding that for supercooled fluids (thick lines) α_2 has a peak corresponding to the end of the plateau of $\langle \Delta x^2 \rangle$, due to the presence of the anomalously mobile particles [14]. For colloidal glasses (thin lines in figure 1(a)), the upturn in $\langle \Delta x^2 \rangle$ is due to ageing, and occurs at a timescale Δt which varies with the time since sample preparation [22]. It is unclear if the motions responsible for the upturn are due to cage rearrangements [14].

Intriguingly, in supercooled colloidal fluids, the motion of these cage-rearranging particles is spatially localized, and the peak of $\alpha_2(\Delta t)$ corresponds to the existence of large clusters of these particles all moving simultaneously [14]. In fact, the positions of mobile particles appear in localized clusters over a range of timescales Δt, and the Δt dependence of the typical cluster

size appears qualitatively similar to the Δt dependence of α_2 [14]. However, interpretations of these observations are difficult, as the details depend on the particular definition of which particles comprise a mobile cluster. In this work we seek to characterize particle motion in a way that does not arbitrarily separate particles into mobile and immobile populations.

We wish to determine how these previously observed clusters of cage-rearranging particles are manifested in correlations of the motion of individual particles. In a dilute suspension of particles, particles have only hydrodynamic interactions, and the correlations between the displacement vectors $\vec{u}$ of two particles should decay as $1/\Delta r$ with increasing separation Δr [23–25]. This result would still hold true for dilute tracers in any homogeneous viscoelastic medium [26, 27]. However, it seems unlikely that our samples are homogeneous on the length scales that we consider; our imaging window has a width of only ∼25 particle diameters. The direct interparticle forces (their electric charge, and steric repulsion) are likely to be as important as hydrodynamic interactions.

Thus, we do not necessarily expect $1/\Delta r$ decay of correlations, especially given the apparently cooperative and localized nature of the cage rearrangement motion. For example, a simulation of hard spheres at large volume fractions found exponential decay [13]. This suggests that particles may rearrange by translating together in a group. One possibility for this group motion is that cage-rearranging particles move in parallel directions [11, 13–15]. An alternate possibility is that *mobility* may be correlated over long distances. Mobility is the magnitude of particle displacements, $u = |\vec{u}|$, sometimes with the average subtracted off ($\delta u \equiv u - \langle u \rangle$). In fact, the previous observations of clusters of anomalously mobile particles are a direct indication that mobility is correlated; simulations have provided evidence that there is a correlation length scale [11, 13]. Correlations of mobility are consistent with both collectively translating regions, and also internal rearrangements within localized regions.

To study these possibilities, we compute two correlation functions from our data: one using $\vec{u}$ and one using the mobility δu [11, 13, 25]. We define

$$S_{\vec{u}}(\Delta r, \Delta t) = \frac{\langle \vec{u}_i \cdot \vec{u}_j \rangle}{\langle u^2 \rangle}, \tag{2}$$

$$S_{\delta u}(\Delta r, \Delta t) = \frac{\langle \delta u_i \delta u_j \rangle}{\langle (\delta u)^2 \rangle}, \tag{3}$$

where the timescale Δt is used to define the displacements $\vec{u}$ and mobility δu. For both formulas, the numerator average is over all pairs of particles i, j with separations Δr, and the denominator average is over all particles.[4,5] The normalization of both of these functions is chosen so that perfectly correlated motion ($\vec{u}_i = \vec{u}_j$ for all particles i, j) corresponds to $S_{\vec{u}} = S_{\delta u} = 1$, perfectly anticorrelated motion ($\vec{u}_i = -\vec{u}_j$) corresponds to $S_{\vec{u}} = -1$, and uncorrelated motion gives $S_{\vec{u}} = S_{\delta u} = 0$. Note that $S_{\delta u}$ measures *fluctuations* of mobility, so

[4] Our function $S_{\vec{u}}$ can be related to the two-particle function described in [25]:

$$D_{\alpha,\beta}(\delta r, \Delta t) = \langle u_i^\alpha u_j^\beta \rangle \tag{4}$$

where α and β indicate the components of the vector displacements to multiply. Thus $D(\delta r, \Delta t)$ can be related to $S_{\vec{u}}(\Delta r, \Delta t)$ as

$$D_{xx} + D_{yy} + D_{zz} = S_{\vec{u}}(\Delta r, \Delta t)\langle |u|^2 \rangle. \tag{5}$$

Note that $\langle |u(\Delta t)|^2 \rangle$ is just the ordinary mean square displacement, and is Δr independent, so to convert from $S_{\vec{u}}(\Delta r, \Delta t)$ to $D(\Delta r, \Delta t)$ is simple.

[5] Our function $S_{\delta u}$ can be related to the two-particle function described in [11], $g_u(\Delta r, \Delta t)$, which is analogous to the static pair correlation function $g(r)$. The static pair correlation function is defined by

$$g(\Delta r) = \frac{1}{4\pi(\Delta r)^2 \langle n \rangle N} \sum_{i, j \neq i} \delta(\Delta r - R_{ij}) \tag{6}$$

either anomalously mobile or anomalously immobile particles would show positive correlation. By examining the Δr dependence of these functions we learn about spatially correlated motion, and by examining the Δt dependence we study the correlated motion seen at different timescales.

To study the Δt dependence of $S_{\vec{u}}$ and $S_{\delta u}$, for convenience we choose a fixed value $\Delta r = \Delta r_{nn}$ for each data set, set by the first maximum of the pair correlation function $g(r)$ (which is slightly larger than at σ, and depends slightly on ϕ, due to the charging of the particles). Pairs of particles with separation Δr_{nn} are nearest neighbours and are strongly correlated due to their close proximity, as will be shown later.

We plot $S_{\vec{u}}(\Delta t, \Delta r_{nn})$ in figure 1(c) and $S_{\delta u}(\Delta t, \Delta r_{nn})$ in figure 1(d). For the supercooled fluids (thick lines), the behaviour of these two functions is dramatically different. $S_{\vec{u}}$ is nearly constant as a function of Δt, whereas $S_{\delta u}$ is small at short lag times, rises to a maximum, and then has a downturn. Strikingly, the Δt dependence of $S_{\delta u}$ is similar to that of the non-Gaussian parameter α_2, which can be seen for three supercooled fluid samples by comparing the thick lines in figures 1(b) and (d). While $S_{\delta u}$ reaches its maximum at slightly larger values of Δt, it appears that the anomalously mobile particles (which cause the increase of α_2) are directly responsible for the increasing correlation measured by $S_{\delta u}$. While the time dependence of the vectorial correlations $S_{\vec{u}}$ is much weaker than for the mobility, there is a slight rise at larger Δt seen in figure 1(c) [13]. It has been conjectured that $S_{\vec{u}}(\Delta t \to \infty)$ should be non-zero, as short-lag-time interparticle correlations will always provide a contribution to $\langle \vec{u}_i \cdot \vec{u}_j \rangle$ even if particles are uncorrelated at longer lag times [13]. This may explain why we do not see a downturn in $S_{\vec{u}}$ at large Δt.

Figures 1(c), (d) also show that at short lag times, $S_{\vec{u}} > S_{\delta u}$, although at the cage-breaking timescales, the opposite is true. These results, along with the similar lag time dependence of α_2 and $S_{\delta u}$, suggest that the cage rearrangements are due to mobility correlations, rather than a strong directional correlation. The implied picture is that regions of cage rearrangements are composed of highly mobile particles, which move in many directions. While the motions of neighbouring particles are somewhat directionally correlated, the cage rearrangements reflect regions of internal restructuring rather than large-scale cooperative translations.

Further confirmation of this picture comes from the volume fraction dependence of the correlation functions, seen in figures 1(c), (d). As ϕ increases towards the glass transition at $\phi_g \approx 0.58$, $S_{\vec{u}}$ changes only slightly, while $S_{\delta u}$ changes dramatically, again similar to the behaviour of α_2. The growth of $S_{\delta u}$ (and non-growth of $S_{\vec{u}}$) indicate that as the glass transition is approached, mobility correlations become increasingly important, while the directional correlations remain virtually unchanged.

which is normalized so that $g(\Delta r) \to 1$ as $\delta r \to \infty$. N is the number of particles in the sample, $\langle n \rangle$ is the number density, and $\delta(\,)$ is the Dirac delta function. Using our notation,

$$g_u(\Delta r, \Delta t) = \frac{\left\langle \sum_{i,j \neq i} u_i u_j \delta(\Delta r - R_{ij}(t)) \right\rangle_t}{4\pi (\Delta r)^2 \langle u \rangle^2 \langle n \rangle N} \tag{7}$$

$$= \frac{\langle u_i u_j \rangle}{\langle u \rangle^2} g(\Delta r) \tag{8}$$

where the angle brackets $\langle\,\rangle_t$ around the sums in the first line indicate a time average, and $\langle u_i u_j \rangle$ is taken over all pairs of particles with separations Δr. It can be shown that

$$\frac{g_u(\Delta r, \Delta t)}{g(\Delta r)} - 1 = \left(\frac{\langle u^2 \rangle}{\langle u \rangle^2} - 1 \right) S_{\delta u}(\Delta r, \Delta t) \tag{9}$$

thus relating our $S_{\delta u}$ with the function g_u; the left-hand side of this equation is equivalent to $\Gamma(\Delta r, \Delta t)$ discussed in [11]. g_u is proportional to $g(\Delta r)$, whereas $S_{\delta u}$ is not.

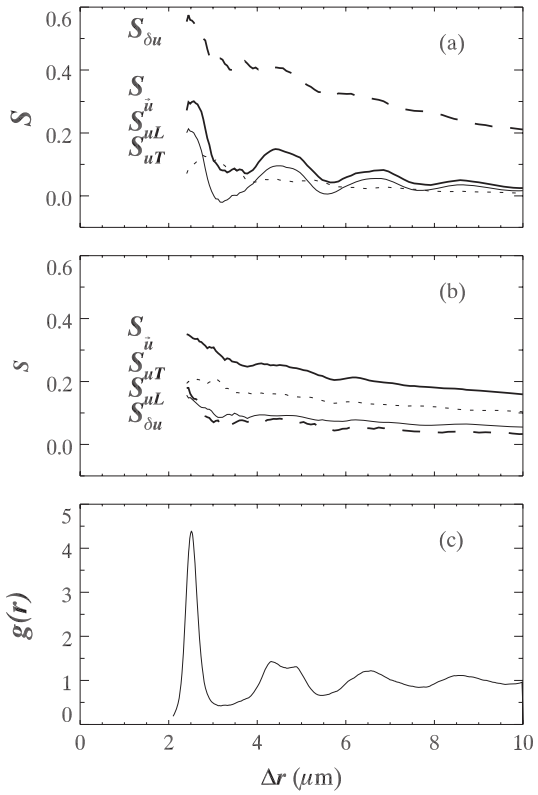

Figure 2. (a) Correlation functions for $\phi = 0.56$ (a supercooled fluid close to the glass transition), with $\Delta t = 2000$ s. (b) Correlation functions for $\phi = 0.62$ (a glass), with $\Delta t = 10\,000$ s. (c) $g(r)$ for the data shown in (a); $g(r)$ is similar for the data shown in (b).

The results are harder to interpret for glassy samples (thin lines in figure 1), due to the ageing of the system. In an ageing system, the properties of the samples depend on the time since the sample was prepared [22]; for example, the increase in $\langle \delta x^2 \rangle$ at large Δt (figure 1(a)) moves to longer Δt as the sample age increases. (The sample age is defined as the time since stirring the sample prior to the start of the experiment. To minimize the effects of ageing for these data, data acquisition was started 5–10 h after stirring the sample, which reliably initiates the ageing [22].) As seen in figures 1(c), (d), any ϕ dependence for the correlated behaviour in glassy samples is unclear. The correlation functions are non-zero due to correlated motion of particles within cages; however, the increases seen in $S_{\vec{u}}$ and $S_{\delta u}$ at large Δt are probably due to the slight motions responsible for ageing [22].

To examine the spatial character of the highly correlated particles occurring at the cage-rearrangement timescales, we study the Δr dependence of these functions, fixing Δt to maximize $S_{\delta u}$ (figure 1(d)). The correlation functions are shown for a supercooled fluid ($\phi = 0.56$) in figure 2(a), indicated by the thick lines. Both functions oscillate, with especially strong oscillations seen in $S_{\vec{u}}$ (thick solid line). Strikingly, these oscillations coincide with oscillations of the pair correlation function $g(r)$, shown in figure 2(c). For example, pairs of particles with separations corresponding to the first peak in $g(r)$ are nearest neighbours, and are the most strongly correlated. This agrees with our earlier work, which found that the pair correlation function $g(r)$ influences the motion of pairs of particles [17]. In fact, comparing $S_{\delta u}$

and $S_{\vec{u}}$ shows that the correlation of the *mobility* of pairs of particles is less sensitive to $g(r)$, whereas the correlation of their *directions* is more sensitive to $g(r)$. This is further evidence that cage rearrangements involve regions of particles with high mobility, although within those regions the directions of the displacements of individual particles are not as strongly correlated, but rather are influenced by $g(r)$. Both simulations of Lennard-Jones particles and of hard spheres saw similar oscillations in spatial correlation functions, but the relationship with $g(r)$ was unclear, as the systems had higher polydispersity than our samples [11, 13] (see footnote 5).

To further examine the correlations in the directions of motion of pairs of particles, we decompose $S_{\vec{u}}$ into longitudinal correlations (correlations of the displacement along the direction of the separation vector $\Delta\vec{r}_{ij}$) and transverse correlations (correlations of the component of the displacement vector perpendicular to $\Delta\vec{r}_{ij}$). Two new functions are defined as:

$$S_{\vec{u}L}(\Delta r, \Delta t) = \frac{\langle u_i^{\mathrm{L}} u_j^{\mathrm{L}} \rangle}{\langle u^2 \rangle} \tag{10}$$

$$S_{\vec{u}T}(\Delta r, \Delta t) = \frac{\langle \vec{u}_i^{\mathrm{T}} \cdot \vec{u}_j^{\mathrm{T}} \rangle}{\langle u^2 \rangle} \tag{11}$$

where $u_i^{\mathrm{L}} = \vec{u}_i \cdot \hat{R}_{ij}$, $u_j^{\mathrm{L}} = \vec{u}_j \cdot \hat{R}_{ij}$, $u_i^{\mathrm{T}} = \vec{u}_i - u_i^{\mathrm{L}} \hat{R}_{ij}$, and $u_j^{\mathrm{T}} = \vec{u}_j - u_j^{\mathrm{L}} \hat{R}_{ij}$. The normalization is chosen so that $S_{\vec{u}} = S_{\vec{u}L} + S_{\vec{u}T}$. $\hat{R}_{ij}$ is a unit vector pointing from particle i to particle j, and the dot products for the u^{L} terms are taken so that two vectors pointed in the same direction correlate positively. These two functions are plotted in figure 2(a) (thin lines). The oscillations of $S_{\vec{u}}$ are almost entirely due to the contribution from $S_{\vec{u}L}$ (thin solid line), indicating that the longitudinal motion is most sensitive to $g(r)$. In fact, the longitudinal correlations of the motions of nearest-neighbour particle pairs are suggestive of 'string-like' motion seen in simulations [28]. However, $S_{\vec{u}L}$ also shows a slight anticorrelation at $\Delta r \approx 3.2$ μm, corresponding to the first minimum of $g(r)$. This indicates that pairs of particles separated by $\approx 1.5\sigma$ are actually more likely to move in antiparallel directions (towards or away from each other), despite their strongly correlated mobility; some evidence for this has also been seen in simulations [12]. The transverse component $S_{\vec{u}T}$ (thin dotted line) has a slight increase near the first minimum of $g(r)$, but otherwise shows little dependence on $g(r)$.

At larger separations, particle motion is still less correlated. If the particles were in a dilute suspension and long-range interactions were solely due to the hydrodynamic behaviour of the solvent, the correlation functions should decrease as $1/\Delta r$. This would also be the case for a homogeneous viscoelastic medium [25], although the localized rearrangements observed previously show that motion in these dense colloidal samples is spatially inhomogeneous [14, 15]. To check this, we plot the correlation functions on semilog and log–log axes in figure 3 for $\phi = 0.56$ at two different timescales. The top right graph shows that the decay is close to $1/\Delta r$ for short timescales; we find similar behaviour for all liquid samples at timescales $\Delta t < 100$ s. The behaviour characteristic of longer timescales relevant for cage rearrangements is shown in the bottom graphs. On the semilog graph, the decays follow straight lines for both functions out to $\Delta r \approx 25$ μm, indicating exponential decay with characteristic length scales $\xi_{\delta u} = 8.5$ μm $= 3.6\sigma$ and $\xi_{\vec{u}} = 6.1$ μm $= 2.6\sigma$. For this sample, the decay lengths vary in the range $\xi_{\delta u} = 7.6 \pm 0.9$ μm and $\xi_{\vec{u}} = 6.7 \pm 0.9$ μm when Δt is varied from 50–5000 s. The exponential decay demonstrates that dense colloidal suspensions on these length scales and timescales do not behave as continuum viscoelastic materials [26, 27].

At large Δr, a downturn is seen in the correlation functions (bottom graphs in figure 3). This is due to a counterflow, similar to what was seen in simulations [13, 29]. This counterflow

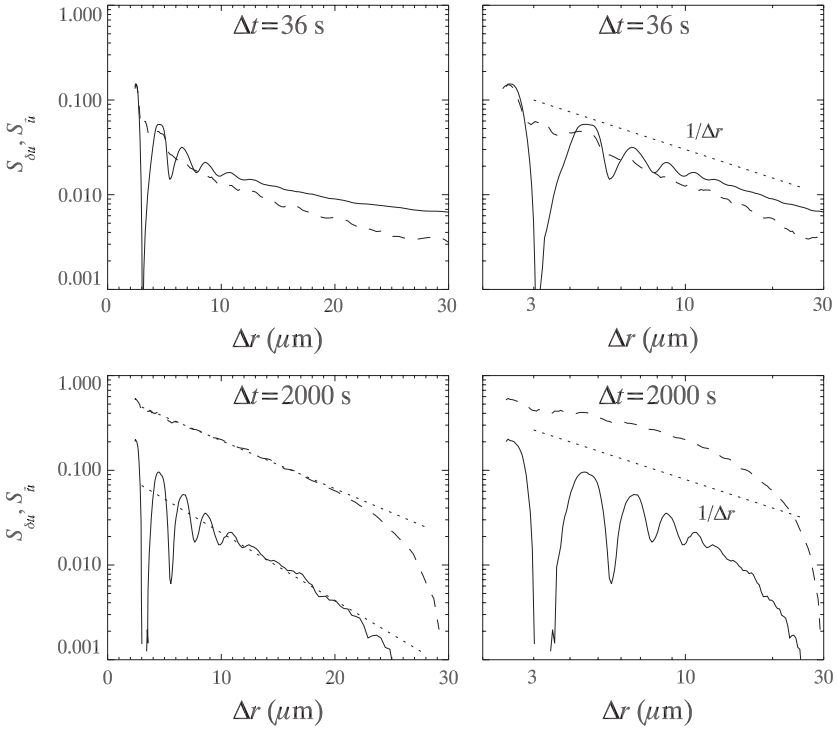

Figure 3. Semilog and log–log plots of $S_{\vec{u}}$ (solid lines) and $S_{\delta u}$ (dashed lines) at two different Δt as indicated, for $\phi = 0.56$, a supercooled fluid. The dotted $1/\Delta r$ lines are drawn as a guide to the eye in the log–log plots. The dotted fit lines shown in the lower left plot have decay lengths $\xi_{\delta u} = 8.5\ \mu$m and $\xi_{\vec{u}} = 6.1\ \mu$m. The downturn at long Δt is not fitted, and is described in the text.

has been interpreted previously as the medium's response to the transient motion of a particle, although it is less clear how this may apply in the case of localized motions [13, 29]. The counterflow may be due to the presence of the cover slip (>30 μm away), although the correlation functions do not change significantly when the data is split into two subsets: one closer to the coverslip and one further away. The counterflow results in a slight anticorrelation in both $S_{\vec{u}}$ and $S_{\delta u}$ at $\Delta r \approx 40\ \mu$m (not shown). In all cases the exponential decay occurs over a decade in Δr before the counterflow cuts off the correlation. At still larger length scales ($\Delta r \gg \xi_{\vec{u}}, \xi_{\delta u}$), the correlation functions must decay as $1/\Delta r$, as on a sufficiently large length scale the colloidal suspension will appear to be homogeneous. However, we do not have data at large enough Δr to see $1/\Delta r$ decay, and at large separations the amplitude of the correlation functions would be quite small and difficult to measure.

To look for a possible growing length scale, we extract the correlation decay lengths for $S_{\vec{u}}$ and $S_{\delta u}$ in samples with different volume fractions, with the results shown in figure 4. The decay lengths increase only slightly as ϕ_g is approached. Within the error bars, $\xi_{\vec{u}}$ is consistent with a constant value $\xi_{\vec{u}} \approx 3\sigma$. $\xi_{\delta u}$ doubles over the range $\phi = 0.46$–0.56, and this is sufficient to account for the increase in the size of clusters of mobile particles seen in previous work [14]; however, we see no evidence in our data for or against a divergence of $\xi_{\delta u}$ at ϕ_g. For these samples, the relaxation timescale grows by a factor of 60 from $\phi = 0.46$ to 0.56, which is a much more dramatic change [17]. Intriguingly, this slight increase in $\xi_{\delta u}$ gives new insight into the ϕ dependence of $S_{\delta u}$ for the supercooled fluids, seen in figure 1(d). If we assume

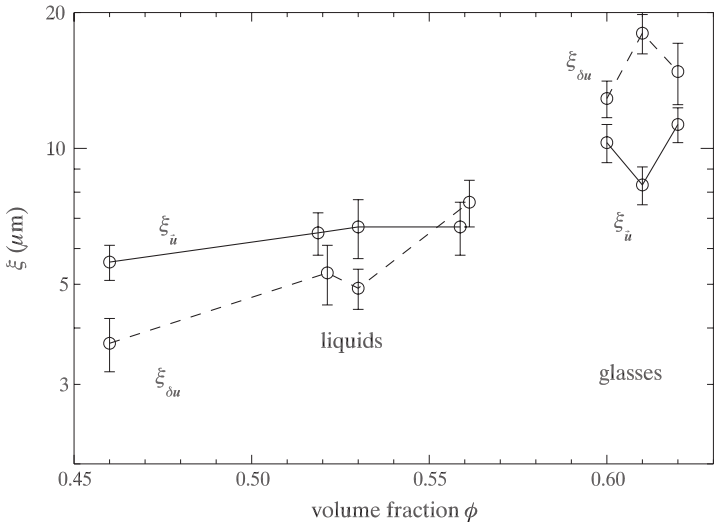

Figure 4. Volume fraction ϕ dependence of the dynamic length scales, for colloidal liquids and glasses. The length scales are determined by a fit to the exponential decay of correlation functions such as those shown in figure 3; the error bars indicate variability in determining the length scales at different Δt s. (The data points for $\phi = 0.52$ and $\phi = 0.56$ are horizontally offset from each other slightly for clarity.)

$S_{\delta u}(\Delta r) = A_\phi(\Delta t)\exp(-\Delta r/\xi_{\delta u})$, we find that the maximum value (with respect to Δt) of $A_\phi(\Delta t)$ is a constant, approximately 0.75 ± 0.05, independent of ϕ. Thus, the increasing height of $S_{\delta u}$ as ϕ increases, seen in figure 1(d), is primarily due to the increase in $\xi_{\delta u}$ and thus an increasing value of $\exp(-\Delta r_{\rm nn}/\xi_{\delta u})$, using the nearest-neighbour separation $\Delta r_{\rm nn}$.

We can compare our length scales $\xi_{\vec{u}}$ and $\xi_{\delta u}$ with length scales obtained from computer simulations of glass-forming systems. The values that we find for $\phi = 0.56$ ($\xi_{\vec{u}} \approx \xi_{\delta u} \approx 3\sigma$) are slightly larger than that seen in simulations of hard spheres ($\xi_{\vec{u}} = 2.3\sigma, \xi_{\delta u} = 1.4\sigma$); the simulations had a higher polydispersity, and thus may have been further from the glass transition at $\phi = 0.56$ [13]. Simulations of Lennard-Jones particles did not notice exponential decay [16], and instead computed a length scale by calculating (in our notation)

$$\xi'(\Delta t) = \left(\frac{\langle u^2\rangle}{\langle u\rangle^2} - 1\right)\int_0^\infty {\rm d}\Delta r\; S_{\delta u}(\Delta r, \Delta t). \tag{12}$$

The term in parenthesis is qualitatively similar to the non-Gaussian parameter α_2, and over the range of liquids shown in figure 4 varies from 0.35 (at $\phi = 0.46$) to 0.70 (at $\phi = 0.56$). We calculate ξ' for our data by using the form $A_\phi(\Delta t)\exp(-\Delta r/\xi_{\delta u})$ for $S_{\delta u}$ with our measured values for A and $\xi_{\delta u}$, and using the value of Δt which maximizes $S_{\delta u}$ (and thus maximizes ξ'). We find that ξ' increases from 0.9 to 4.1 μm $\approx 0.4\sigma$–1.7σ as the glass transition is approached. These values are larger than those seen in the simulation (0.05–0.32 in Lennard-Jones units) [16].

Earlier work has seen evidence that structural properties of the sample are slightly correlated with particle mobility [17, 30]. This then suggests that the exponential length scales seen in the correlation functions may relate to spatial correlations of structural properties. We have computed a spatial correlation function $S_{\delta V}$ similar to $S_{\delta u}$ (3), except looking at fluctuations δV of the Voronoi volume V of each particle. The Voronoi volume is a geometric way of partitioning space, so that each particle claims the volume that is closer to its centre

than to the centre of any other particle. Particles with slightly larger Voronoi volumes are, in some sense, seeing a slightly smaller local volume fraction, and this is correlated with a slightly enhanced mobility [17]. The correlations $S_{\delta V}$ do decay exponentially (not shown), with a length scale of 5.7–6.3 μm for the four liquid samples that we consider ($\sim 2.5\sigma$). Strikingly, we see no clear volume fraction dependence of this length scale. Furthermore, this length scale is quite similar to the length scales seen for $S_{\vec{u}}$. The lack of a clear connection to the length scale for mobility ($\xi_{\delta u}$) suggests that the correlation between the structure and the mobility, while present, is not the entire story; the cooperative motions are influenced by more factors than just the local volume [30, 31].

For the glassy samples, the behaviour is strikingly different. As discussed before, our glassy samples are ageing, although for the duration of the experiment, little ageing occurs. (We consider samples with a large age $t_w = 3 \times 10^4$ s and timescales $\Delta t \leqslant t_w$.) For our data, and for lag times $\Delta t < 5000$ s, almost all particle motion consists of particles moving back and forth within their cages. $S_{\vec{u}}$ and $S_{\delta u}$ have a low amplitude, as shown in figures 1(c), (d) and figure 2(b), indicating that most of the motion is uncorrelated. For the glassy samples, $S_{\vec{u}} > S_{\delta u}$, similar to the liquids at small Δt. Figure 2(b) also shows that the correlation functions oscillate much less, and thus the local structure [$g(r)$] has a only a minor role for glasses. Another intriguing difference is that $S_{\vec{u}T} > S_{\vec{u}L}$, indicating that fluctuations in the transverse directions are more strongly correlated than in the longitudinal direction.

The correlated motion that is present in the glasses, while of small amplitude, is rather long-ranged. Similar to the supercooled fluids, the correlation functions for glasses show exponential decay over a range of timescales Δt. The length scales for the decay are plotted in figure 4. They are significantly larger than the length scales associated with the supercooled fluids; for the glasses, $\xi_{v,\delta v} = 8$–$20\ \mu\text{m} \approx 3.5\sigma - 8.5\sigma$. The data shown in figure 4 also indicate that the scalar correlation lengths $\xi_{\delta u}$ are noticeably larger than the vector correlation lengths $\xi_{\vec{u}}$, a trend which is the opposite to that of the liquids. The existence of this long-range correlation is sensible, given that the glasses are more densely packed: while most motion is localized and uncorrelated, particles can move slightly if there is long-range cooperation, even if they then move back (in order that there are no rearrangements). At present, however, it is unclear if these correlation length scales correspond to the intrinsic motion of the frozen glassy system, or if they are connected with the ageing process [22]. The previous observations that clusters of 'mobile' particles are smaller is consistent with the low amplitude of the correlations [14, 22].

Unlike the correlated motion in glasses, the structural correlations in the glassy samples are not long-ranged. The length scale for $S_{\delta V}$, the correlation function of the fluctuations of Voronoi volumes, stays comparable to that of the liquids ($\xi_{\delta V} \sim 5.9$–$7.7\ \mu$m for the glasses). While there is very little change of this length scale with ϕ, we do note that the two samples with the largest values of $\xi_{\delta V}$ correspond to the same two samples with the largest values of $\xi_{\vec{u}}$, again suggesting a connection between the structure and correlated particle motion [32].

4. Conclusions

By measuring the positions of several thousand particles over several hundred time steps, we have found that particle motion is correlated over distances of 3–4 particle diameters. In particular, particles undergoing cage rearrangements have anomalously large displacements, and these are highly spatially correlated. We note that the largest degree of correlation exists at the timescales corresponding to cage rearrangements, but that our observations do not preclude the sample from acting differently at very long timescales. All of our data is taken at timescales $\Delta t < \tau_\alpha$, so we are not able to quantify the behaviour on timescales corresponding to alpha relaxation.

At timescales similar to the cage-rearrangement timescale, the correlations decay exponentially with separation Δr. At very large Δr, we would expect the correlations to recover a $1/\Delta r$ dependence, as predicted for homogeneous viscoelastic media [26, 27], at any timescale. This dependence is seen at short timescales in our data (figure 3), suggesting that the instantaneous response may be more continuum-like [33]. This is sensible; in such short timescales, $\Delta t \ll \tau_\alpha$, so these motions are not related to dynamical heterogeneities, and do not lead to flow of the sample. Rather, these are small-amplitude affine deformations. It is intriguing that, on the cage-rearrangement timescales, our image volume is not large enough to see the $1/\Delta r$ behaviour, suggesting that the appropriate coarse-graining length scale is bigger than $\sim 25\sigma$.

The differing behaviour of the two correlation functions that we examine suggests that these rearrangements are composed of regions of mobile particles (particles with large displacements), but that the motions involve particles moving in many directions, rather than all of the particles moving in one coherent direction. This is especially clear as the correlations between the directions of motion of particles ($S_{\vec{u}}$) strongly depend on the pair correlation function; within a group of mobile particles, their motions are often strongly directionally correlated, but also frequently not directionally correlated. This is consistent with particles moving in necklace-like loops, for example, as seen in [28], and the mixing motions described in [17].

The correlations become increasingly long-ranged as the glass transition is approached, as seen in two new correlation lengths $\xi_{\delta u}$ and $\xi_{\vec{u}}$. This suggests that rearrangements involving regions consisting of a small number of particles become difficult or impossible as the volume fraction increases, which would explain the growth of the viscosity as the glass transition is approached. The size of these regions, quantified by the two correlation lengths $\xi_{\vec{u}}$ and $\xi_{\delta u}$, are direct experimental evidence for dynamical length scales near the glass transition.

Acknowledgments

We thank L Berthier, B Doliwa, U Gasser, and S C Glotzer for helpful discussions. We thank A Schofield for providing our colloidal samples. This work was supported by the US National Science Foundation (NSF) (DMR-0239109, DMR-0602584) and the Harvard Materials Research Science and Engineering Center (MRSEC) (NSF DMR-0213805).

References

[1] Angell C A 2000 *J. Phys.: Condens. Matter* **12** 6463
[2] Ediger M D, Angell C A and Nagel S R 1996 *J. Phys. Chem.* **100** 13200
[3] Adam G and Gibbs J H 1965 *J. Chem. Phys.* **43** 139
[4] Kivelson S A, Zhao X, Kivelson D, Fischer T M and Knobler C M 1994 *J. Chem. Phys.* **101** 2391
[5] Götze W and Sjögren L 1992 *Rep. Prog. Phys.* **55** 241
[6] Ngai K L and Rendell R W 1998 *Phil. Mag.* B **77** 621
[7] Parisi G 1999 *J. Phys. Chem.* B **103** 4128
[8] Garrahan J P and Chandler D 2003 *Proc. Natl Acad. Sci.* **100** 9710
[9] Ediger M D 2000 *Annu. Rev. Phys. Chem.* **51** 99
[10] Alcoutlabi M and McKenna G B 2005 *J. Phys.: Condens. Matter* **17** R461
[11] Donati C, Glotzer S C and Poole P H 1999 *Phys. Rev. Lett.* **82** 5064
[12] Flenner E and Szamel G 2006 *J. Phys.: Condens. Matter* **19** 205125 (*Preprint* cond-mat/0608398)
[13] Doliwa B and Heuer A 2000 *Phys. Rev.* E **61** 6898
[14] Weeks E R, Crocker J C, Levitt A C, Schofield A and Weitz D A 2000 *Science* **287** 627
[15] Kegel W K and van Blaaderen A 2000 *Science* **287** 290
[16] Poole P H, Donati C and Glotzer S C 1998 *Physica* A **261** 51

[17] Weeks E R and Weitz D A 2002 *Phys. Rev. Lett.* **89** 095704
[18] Dinsmore A D, Weeks E R, Prasad V, Levitt A C and Weitz D A 2001 *Appl. Opt.* **40** 4152
[19] Pusey P N and van Megen W 1986 *Nature* **320** 340
[20] Pusey P N and van Megan W 1987 *Phys. Rev. Lett.* **59** 2083
[21] Gasser U, Weeks E R, Schofield A, Pusey P N and Weitz D A 2001 *Science* **292** 258
[22] Courtland R E and Weeks E R 2003 *J. Phys.: Condens. Matter* **15** S359
[23] Batchelor G K 1976 *J. Fluid Mech.* **74** 1
[24] Crocker J C 1997 *J. Chem. Phys.* **106** 2837
[25] Crocker J C *et al* 2000 *Phys. Rev. Lett.* **85** 888
[26] Levine A J and Lubensky T C 2000 *Phys. Rev. Lett.* **85** 1774
[27] Levine A J and Lubensky T C 2001 *Phys. Rev.* E **63** 041510
[28] Donati C *et al* 1998 *Phys. Rev. Lett.* **80** 2338
[29] Alder B J and Wainwright T E 1970 *Phys. Rev.* A **1** 18
[30] Conrad J C, Starr F W and Weitz D A 2005 *J. Phys. Chem.* B **109** 21235
[31] Widmer-Cooper A, Harrowell P and Fynewever H 2004 *Phys. Rev. Lett.* **93** 135701
[32] Cianci G C, Courtland R E and Weeks E R 2006 *Solid State Commun.* **139** 599
[33] Habdas P, Anderson D, Hay J and Weeks E R 2007 in preparation